



Annual temperatures during the last 2485 years in the mid-eastern Tibetan Plateau inferred from tree rings

LIU Yu^{1,3†}, AN ZhiSheng¹, Hans W. LINDERHOLM², CHEN DeLiang², SONG HuiMing¹, CAI QiuFang¹, SUN JunYan¹ & TIAN Hua^{1,4}

¹ State Key Laboratory of Loess and Quaternary Geology, Institute of Earth Environment, Chinese Academy of Sciences, Xi'an 710075, China;

² Regional Climate Group, Department of Earth Sciences, University of Gothenburg, 40530 Gothenburg, Sweden;

³ Department of Environment Science and Technology, School of Human Settlements and Civil Engineering, Xi'an Jiaotong University, Xi'an 710049, China;

⁴ Graduate School of the Chinese Academy of Sciences, Beijing 100049, China

By combining living trees and archaeological wood, the annual mean temperatures were reconstructed based on ring-width indices of the mid-eastern Tibetan Plateau for the past 2485 years. The climate variations revealed by the reconstruction indicate that there were four periods to have average temperatures similar to or even higher than that mean of 1970 to 2000 AD. A particularly notable rapid shift from cold to warm, we call it the “Eastern Jin Event”, occurred from 348 AD to 413 AD. Calculation results show that the temperature variations over the mid-eastern Tibetan Plateau are not only representative for large parts of north-central China, but also closely correspond to those of the entire Northern Hemisphere over long time scales. During the last 2485 years, the downfall of most major dynasties in China coincides with intervals of low temperature. Compared with the temperature records in other regions of China during the last 1000 years, this reconstruction from the Tibetan Plateau shows a significant warming trend after the 1950s.

mid-eastern Tibetan Plateau, tree rings, temperature variations, dynasty's downfall

Tree rings are widely used as climate proxies and, due to their large geographical distribution (except the tropics) and sensitivity to climate variations, they are possible to provide large-scale paleoclimate information on annual to centennial time scales^[1–7]. It has been suggested that the Tibetan Plateau is one of the regions in the world that are sensitive to global climate change^[8]. This region may provide both regional and global-scale climatic signals. The high-altitude and continental nature of the Tibetan Plateau makes the region highly suitable for high-resolution and long-term studies of past climate variability using tree-ring data.

Indeed, several dendroclimatological studies have been carried out on the Tibetan Plateau, but these mainly focused on precipitation^[9–13] and only a few on temperatures^[14–17]. However, so far it has no temperature

records exceeding 2000 years with annual-resolution in this region. In contrast to eastern China, where past temperatures have been reconstructed for the last 1000 years using historical documents^[18], there is a general lack of paleo-temperature information of high-resolution from the sensitive regions of western China.

Here we present a 2485-year reconstruction of annual temperatures based on a combination of living trees and archaeological wood from the northeastern Tibetan Plateau, and obtain some new results.

Received July 25, 2008; accepted December 22, 2008; published online February 3, 2009
doi: 10.1007/s11430-009-0025-z

†Corresponding author (email: liuyu@loess.llqg.ac.cn)

Supported by National Natural Science Foundation of China (Grant Nos. 40525004, 40599420, 40890051), National Basic Research Program of China (Grant Nos. 2007BAC30B00, 2004CB720200, 2006CB400503) and the Swedish International Development Cooperation Agency (SIDA, Grant to Hans W. Linderholm)

1 Data and method

1.1 Sampling and chronology

The average elevation of the studied area is about 3300 m (Figure 1). In the region, the annual climatic cycle is characterized by a monsoonal pattern with wet and dry seasons. During the summer season in the Tibetan Plateau, the climate is relatively mild and wet due to the thermal low pressure, and during the winter season, cold high pressure predominates and the weather is dry^[19]. The meteorological data show that the annual mean temperature is about 3°C, and annual rainfall is 180–200 mm in the past 40 years.

Qilian juniper (*Sabina przewalskii* Kom.), an endemic Chinese species, was used for dendroclimatological study. It grows in very cold, arid environments with poor soil development, and is mainly distributed around the desert of the Qaidam Basin in western China.

Living tree samples were taken from Wulan and Dulan. In Wulan, samples from 25 living trees were collected from a valley. Dulan samples are from the ref. [13]. The tree-ring width chronology was created following the standard procedures. All the samples were surfaced, cross-dated and measured^[20]. Ring-width series of all trees were standardized to remove the age-related effects. To preserve the long-term climatic fluctuations (low-frequency signals) in the series, we used a conservative detrending method. In the process, we selected negative exponential curves or straight-lines to fit each ring-width measurement series, and combined them into a single chronology using a bi-weight robust estimate of the mean^[21]. The living tree chronology spans from 400 AD to 2000 AD. The statistical characteristics of living tree chronology are shown in the second column in Table 1.

Archaeological woods were sampled from Dulan, 100 km south of Wulan (Figure 1). More than 180 wood

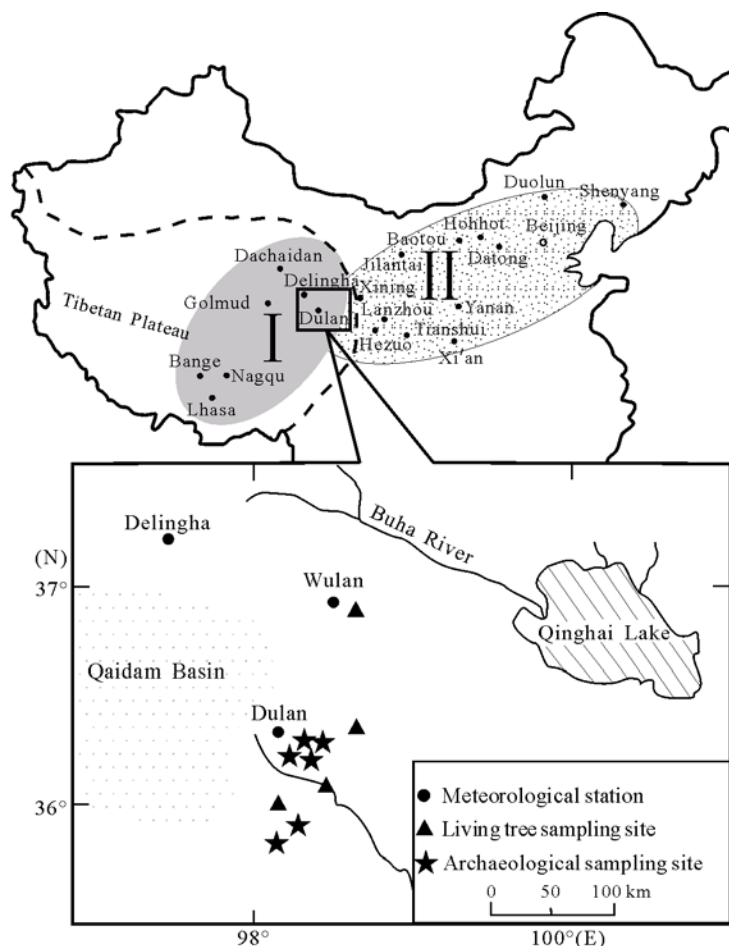


Figure 1 Tree-ring sampling sites and meteorological stations used. Region I represents the mid-eastern Tibetan Plateau, and it contains 7 meteorological stations (including Dachaidan, Delingha, Dulan, Golmud, Bange, Nagqu and Lhasa). Region II represents the central-northern China, and it contains 13 meteorological stations (including Shenyang, Duolun, Beijing, Hohhot, Baotou, Datong, Jilantai, Xining, Lanzhou, Yan'an, Xi'an, Tianshui and Hezuo). The dashed line is the profile of the Tibetan Plateau.

Table 1 Statistical characteristics of the living and the archaeological wood chronologies

Statistical item	Living tree	Archaeological wood
Mean sensitivity	0.16	0.2
Standard deviation	0.19	0.24
First order autocorrelation	0.42	0.51
Mean correlation among all series	0.26	0.35
Mean correlation among trees	0.26	0.34
Mean correlation with trees	0.35	0.44
Variance in PC1 (%)	28.49	36.5
Expressed population signal (EPS)	0.95	0.96
Ratio of signal/noise	20.25	26.21
First year of SSS>0.75 (number of trees)	989 AD (9)	404 BC (6)
First year of SSS>0.80 (number of trees)	1007 AD (12)	401 BC (8)

samples of juniper trees (most are tree discs, and a few are cores) were collected from six tombs, built during the Tang Dynasty 618–907 AD^[22]. The archaeological tree-ring chronology extends from 484 BC to 804 AD. The statistical characteristics of the archaeological chronology display in the third column in Table 1. To keep more low-frequency climatic signals, the standard (STD) chronologies were used for both the living and the archaeological trees. The entire chronology spans 2485 years, from 484 BC to 2000 AD, by combining the living and the archaeological trees.

1.2 Climatic data and correlation function analysis

To avoid the local climatic signals by using only a single meteorological station, we used seven stations on the mid-eastern Tibetan Plateau (METP, region I in Figure 1) to do the regional climatic response analysis. Seven stations are: Dachaidan, Delingha, Dulan, Golmud, Bange, Nagqu and Lhasa. The correlation analysis shows that both the monthly and annually mean temperatures among these stations are significantly correlated ($P<0.0001$). The correlations of the STD chronology (combined Wulan and Dulan living trees) with the monthly mean temperatures and monthly total precipitations of these seven meteorological stations show that the mean temperatures of two periods are highly correlated. One period is from prior September to current March (T_{93}), which is similar to Zhu et al.'s result^[17], and the other is the previous year (from prior January to prior December, $T_{\text{ann-1}}$). All correlations between the STD chronology and $T_{\text{ann-1}}$ of other six stations are higher than 0.57 ($P<0.0001$), except with Dulan $r=0.44$ ($P<0.007$) (Table 2). We therefore use the arithmetic average of the monthly temperatures and precipitations of the seven meteorological stations for correlation analysis (Figure 2).

Table 2 Correlations between the ring-width index and the observed instrumental temperature data of previous year (prior January to prior December) from each of seven meteorological stations in Region I

Meteorological station in region I	Correlation r (P)
Dachaidan (1958–2000)	0.57 (0.0001)
Delingha (1957–2000)	0.58 (0.0001)
Dulan (1955–2000)	0.44 (0.007)
Golmud (1957–2000)	0.66 (0.0001)
Bange (1958–2000)	0.73 (0.0001)
Nagqu (1956–2000)	0.65 (0.0001)
Lhasa (1956–2000)	0.64 (0.0001)
Averaged temperature within 7 stations (1958–2000)	0.692 (0.0001)

In Figure 2, the STD chronology is significantly and positively correlated with almost each month temperature of seven meteorological stations in the previous year. The correlations between the chronology and the monthly mean temperature in prior months of January, February, March, October, November and December are higher than 0.51 ($P<0.0001$), and even higher with prior November with $r=0.63$ ($P<0.0001$). The correlations with prior May, June and July are close to 99% confidence level. However, in current year, the chronology is only significantly correlated with January and March, and there are no significant correlations with other month of the current year. After combining different months, the highest correlations is given to the whole previous year ($T_{\text{ann-1}}$), with $r=0.692$ ($P<0.0001$), secondly given to prior September to current March (T_{93}), with $r=0.686$ ($P<0.0001$), and thirdly from prior July to current June (T_{76}), with $r=0.57$ ($P<0.0001$).

For precipitation, the correlations between the STD chronology and average precipitation of the seven meteorological stations are lower than temperatures. The chronology is significantly correlated with the precipitation in April, July and September of the previous year and January, March, June of the current year at 99%

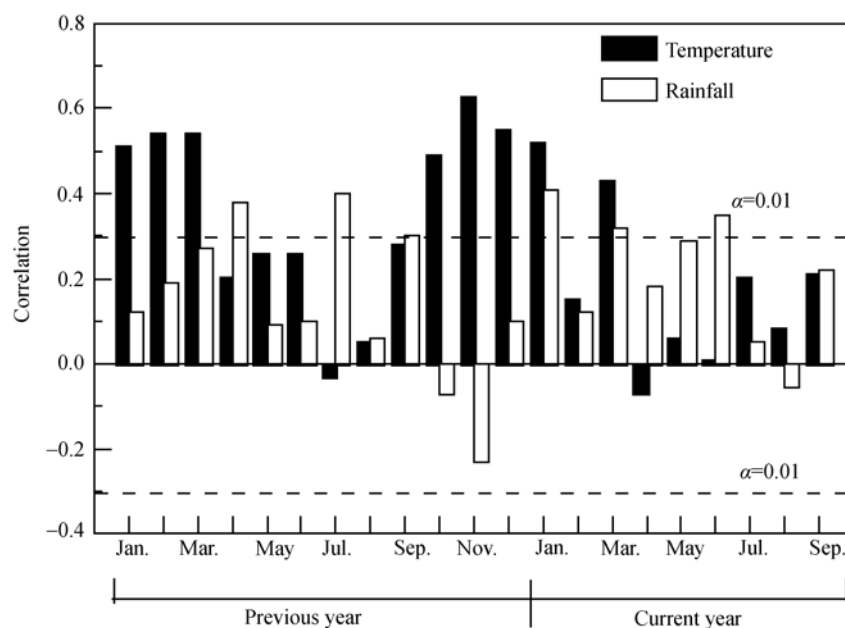


Figure 2 The correlation analysis between the STD chronology and monthly mean temperatures and monthly total precipitations of seven stations in the Region I (1958–2000 AD).

confidence level. After combination of months, the correlations between the chronology and the precipitation of the whole previous year (P_{1-12}) is 0.43 ($P<0.0001$), from prior September to current March (P_{93}) is 0.33 ($P<0.0001$), from prior July to current June (P_{76}) is 0.52 ($P<0.0001$). These results are consistent with earlier findings^[12,13].

Above analyses prove that the living tree chronology from Wulan and Dulan mainly responds to a large-scale temperature variations, but limits to regional precipitation. It is hard to obtain the temperature signals if only using the Dulan single meteorological data for analyses. This is why only the local precipitation signals were captured and no temperature in the previous studies^[9,10,13].

1.3 Transfer function and the temperature reconstruction for the past 2485 years

Although the correlation between the ring-width chronology and the mean temperature from prior September to current March (T_{93}) is 0.686 ($P<0.0001$), it is still lower than that between the chronology and the mean temperature of the entire previous year ($T_{\text{ann-1}}$) with $r=0.692$ ($P<0.0001$). It is worth noting that T_{93} and $T_{\text{ann-1}}$ are significantly correlated with $r=0.88$ ($P<0.0001$, 1958–2006). Thus, we decided to reconstruct the annual mean temperatures of the previous year ($T_{\text{ann-1}}$) for the mid-eastern Tibetan Plateau (Region I) for the past

2485 years.

The transfer function is as follows:

$$T_{\text{ann-1}} = 1.804W + 0.33, \quad (1)$$

where $T_{\text{ann-1}}$ is the annual mean temperatures of previous year, and W is the associated tree-ring chronology index for the year. In the model (1), $n=43$, $r=0.692$, $F=37.72$, standard deviation is 0.47, and $P<0.0001$. During the calibration period 1958–2000 AD, the reconstruction tracks the observation very well with the explained variance 47.9% (46.6% after adjusted for loss of degrees of freedom) in the temperature data (Figure 3). Due to the shortness of the meteorological data set, Bootstrap and Jack-knife statistical methods^[23] (Table 2) were adopted to verify the model (1). The idea behind the bootstrap method is that the available observations of a variable contain the necessary information to construct an empirical probability distribution of any statistic of interest. The bootstrap can provide standard errors of statistical estimators even when no theory exists^[21]. Jack-knife involves the calculation of the correlation of the time series after removing the values for one year progressively throughout the whole time period.

After 45 iterations during the bootstrap process, we obtained results equivalent to those of the Jack-knife method. All values of r , R^2_{adj} , standard deviation (σ), F value, t value, P value and Durbin-Watson statistics are close to the values found on the total data set (Table 3). These analyses indicate that the calibration regression

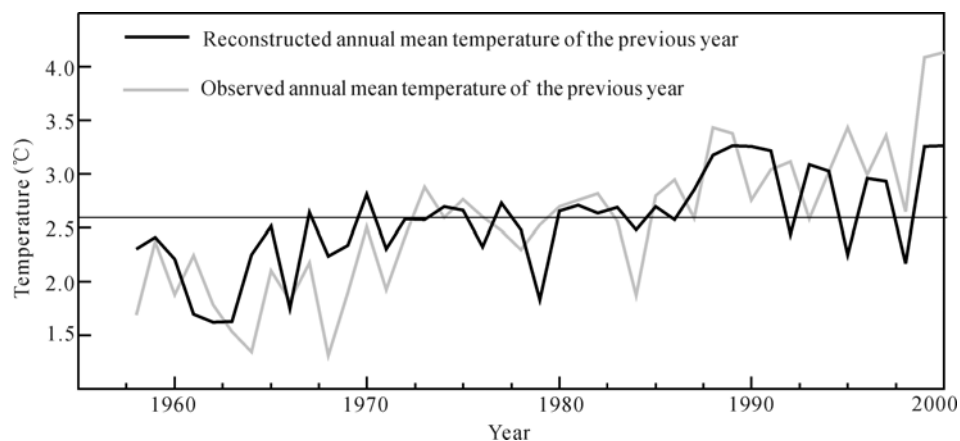


Figure 3 Comparison between observed and tree-ring estimated previous year mean temperatures of the mid-eastern Tibetan Plateau region. Horizontal line represents the mean of 1958–2000 AD.

Table 3 The verification results of the bootstrap and Jack-knife methods^[23] for the reconstructed annual mean temperature of the previous year in the mid-eastern Tibetan Plateau

Calibration (1958–2000 AD)		Verification (1958–2000 AD)	
Statistical item		Jackknife Mean (range)	Bootstrap (45 iterations) Mean (range)
r	0.692	0.69 (0.67–0.74)	0.66 (0.42–0.79)
R^2	0.479	0.486 (0.45–0.79)	0.444 (0.18–0.62)
R^2_{adj}	0.466	0.466 (0.43–0.53)	0.43 (0.16–0.62)
Standard deviation (σ)	0.47	0.47 (0.44–0.48)	0.48 (0.36–0.60)
F	37.72	36.89 (32.14–47.29)	34.73 (8.86–66.87)
t	6.14	6.07 (5.67–6.88)	5.80 (2.98–8.18)
P	0.0001	0.0001	0.0001
Durbin-Watson	1.41	1.42 (1.26–1.54)	1.36 (0.91–1.72)

model is stable and reliable, and consequently the previous annual mean temperatures are reconstructed for the period 484 BC to 2000 AD (Figure 4(b)). Although the transfer function in this paper is based on 43 years observation data, it also can be applied in the past 2485 years according to “the uniformitarian principle”^[24].

2 Results and discussion

2.1 The large-scale representative and uncertainty of the reconstructed temperature

Calculations show that the instrumental temperature records between the mid-eastern Tibetan Plateau (Region I in the Figure 1) and north-central China (Region II in the Figure 1) are significantly correlated (Table 4). The annual mean temperatures of the seven meteorological stations in Region I are significantly correlated with the temperatures of each of the 13 meteorological stations in Region II (including Shenyang, Beijing, Hohhot, Baotou, Datong, Jilantai, Xining, Lanzhou, Yan’an, Xi’an, Tianshui and Hezuo). The ring-width-based reconstructed annual mean temperature is also significantly

correlated with the temperatures of each of the 13 meteorological stations in Region II at 95% confidence level (except with Xi’an and Datong at 90%). All calculations indicate that the tree-ring temperature records represent a large scale, extending from the mid-eastern Tibetan Plateau to north-central China.

During the last millennium, the temperature reconstruction on the mid-eastern Tibetan Plateau can be well compared with previous published temperature reconstructions using historical documents from northern and eastern China^[18] and $\delta^{18}\text{O}$ from Dunde ice core^[25] which contains temperature signals (Figure 5(a)). The twentieth century warming is much more conspicuous in the mid-eastern Tibetan Plateau than in other regions in China since the 1950s.

Moreover, it is evident that there is a strong association, especially on multidecadal time scales, between the mid-eastern Tibetan Plateau temperatures and those reconstructed for the Northern Hemisphere (there are four curves longer than 1000 years among them). Table 5 shows the annual correlations between the mid-eastern Tibetan Plateau temperature and other temperature

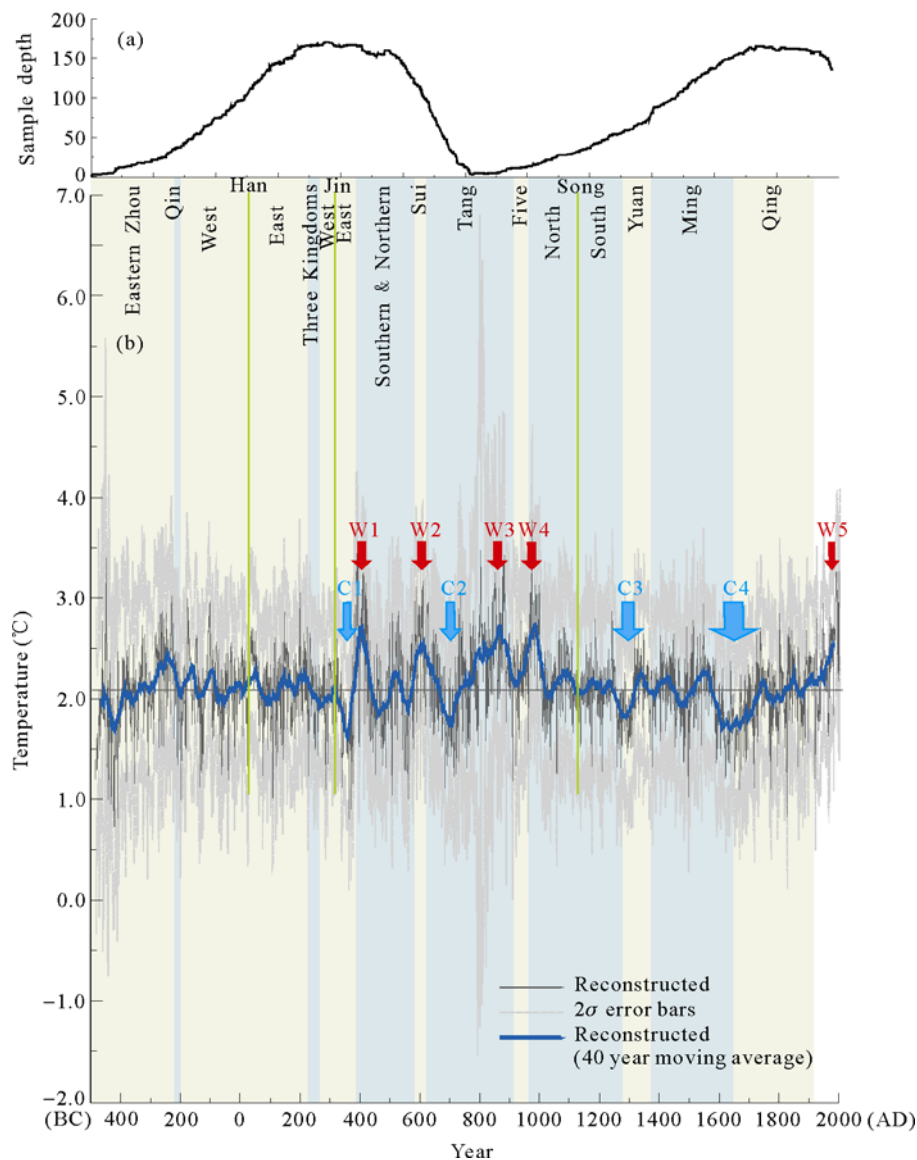


Figure 4 (a) The sample depths. (b) The reconstructed temperature over the mid-eastern Tibetan Plateau from 484 BC to 2000 AD (thin lines) with 2σ error bars (dashed lines). The horizontal line is the mean of 484 BC–2000 AD, and the thick line is the 40-year moving average. The colored areas indicate periods covered by different Dynasties. W1 to W5 are the warm periods, and C1 to C4 are the cold intervals.

Table 4 Correlations between each of 13 meteorological stations in Region II and the mean temperature of Region I (mean of 7 stations on the mid-eastern Tibetan Plateau), and tree-ring-based reconstructed temperature ($T_{\text{ann-1}}$)

Meteorological stations in Region II	Correlation with mean temperature ($T_{\text{ann-1}}$) from 7 stations in Region I (1958–2000 AD) r (P)	Correlation with tree-ring temperature reconstruction ($T_{\text{ann-1}}$) r (P , interval)
Shenyang	0.48 (0.001)	0.33 (0.02, 1952–2000)
Duolun	0.62 (0.0001)	0.36 (0.01, 1954–2000)
Beijing	0.44 (0.003)	0.31 (0.03, 1952–2000)
Baotou	0.68 (0.0001)	0.41 (0.004, 1952–2000)
Hohhot	0.70 (0.0001)	0.44 (0.002, 1952–2000)
Datong	0.59 (0.0001)	0.26 (0.09, 1956–2000)
Jilantai	0.61 (0.0001)	0.31 (0.04, 1956–2000)
Yan'an	0.69 (0.0001)	0.37 (0.008, 1952–2000)
Hezuo	0.82 (0.0001)	0.53 (0.0001, 1959–2000)
Tianshui	0.67 (0.0001)	0.32 (0.03, 1952–2000)
Xi'an	0.50 (0.001)	0.24 (0.1, 1952–2000)
Lanzhou	0.76 (0.0001)	0.48 (0.0001, 1952–2000)
Xining	0.52 (0.0001)	0.39 (0.007, 1955–2000)

curves in different time spans for the Northern Hemisphere. For instance, the correlation between the METP temperature and that from ref. [26] is 0.29 during 200–1980 AD ($P<0.0001$, $n=1781$), with $r=0.42$ during 1600–1980 AD ($P<0.0001$, $n=381$). The correlation between the METP and Esper et al. temperature curves is 0.36 during 831–1992 AD ($P<0.0001$, $n=1162$), and 0.48 during 1600–1992AD ($P<0.0001$, $n=393$). Calculations also show that correlations with each curve are getting higher after 1600 AD than before (Table 5).

The correlations are much higher when all curves were smoothed by 40-year moving average (Table 6). For example, the correlation between the mid-eastern Tibetan Plateau and ref. [26] reaches to 0.58 during 220–1961 AD ($P<0.0001$, $n=1742$), and 0.76 during 1600–1961 AD ($P<0.0001$, $n=362$). The correlation between the METP and Briffa's^[3] temperature is high to

0.66 during 1020–1973 AD ($P<0.0001$, $n=954$), and 0.76 during 1600–1973 AD ($P<0.0001$, $n=374$). After 1600 AD, the METP correlated with Esper et al.^[5] high to 0.83 ($P<0.0001$, $n=374$, 1600–1973 AD), with ref. [6] to 0.79 ($P<0.0001$, $n=360$, 1600–1959 AD), and even high to 0.88 with ref. [27] ($P<0.0001$, $n=341$, 1600–1940 AD).

These calculation results indicate that the temperature variations on the mid-eastern Tibetan Plateau are roughly synchronous to that of the Northern Hemisphere (Figure 5(b)). There are especially close agreements with the temperature curves shown by Esper et al.^[5], Briffa^[3] and Mann et al.^[26]. A stand-out feature in the METP temperature reconstruction is the strong multidecadal variability between ca. 400 and 1000 AD, which is not obvious in other records. Other Northern Hemisphere temperature curves are relatively stable without

Table 5 The correlations between the mid-eastern Tibetan Plateau annual mean temperature and the other Northern Hemisphere temperature curves in different time spans

	Correlation with the mid-eastern Tibetan Plateau (this paper)
Jones et al. ^[1]	0.21 ($P<0.0001$, $n=992$, 1000–1991 AD)
	0.30 ($P<0.0001$, $n=392$, 1600–1991 AD)
Briffa ^[3]	0.26 ($P<0.0001$, $n=994$, 1000–1993 AD)
	0.35 ($P<0.0001$, $n=394$, 1600–1993 AD)
D'Arrigo et al. ^[4]	0.18 ($P<0.0001$, $n=1737$, 264–2000 AD)
	0.16 ($P<0.001$, $n=401$, 1600–2000 AD)
Esper et al. ^[5]	0.36 ($P<0.0001$, $n=1162$, 831–1992 AD)
	0.48 ($P<0.0001$, $n=393$, 1600–1992 AD)
Moberg et al. ^[6]	0.16 ($P<0.0001$, $n=1979$, 1–1979 AD)
	0.34 ($P<0.0001$, $n=380$, 1600–1979 AD)
MJ ^[26]	0.29 ($P<0.0001$, $n=1781$, 200–1980 AD)
	0.42 ($P<0.0001$, $n=381$, 1600–1980 AD)
BO ^[27]	0.26 ($P<0.0001$, $n=559$, 1402–1960 AD)
	0.29 ($P<0.0001$, $n=361$, 1600–1960 AD)

Table 6 The correlations between the mid-eastern Tibetan Plateau and the other Northern Hemisphere temperature curves in different time intervals^{a)}

	Correlation with the mid-eastern Tibetan Plateau _40 (this paper)
Jones_40 ^[1]	0.54 ($P<0.0001$, $n=952$, 1020–1971 AD)
	0.65 ($P<0.0001$, $n=372$, 1600–1971 AD)
Briffa_40 ^[3]	0.66 ($P<0.0001$, $n=954$, 1020–1973 AD)
	0.76 ($P<0.0001$, $n=374$, 1600–1973 AD)
D'Arrigo_40 ^[4]	0.27 ($P<0.0001$, $n=1698$, 283–1980 AD)
	0.18 ($P<0.001$, $n=382$, 1600–1981 AD)
ESP_40 ^[5]	0.60 ($P<0.0001$, $n=1123$, 851–1973 AD)
	0.83 ($P<0.0001$, $n=374$, 1600–1973 AD)
Moberg_40 ^[6]	0.38 ($P<0.0001$, $n=1939$, 21–1959 AD)
	0.79 ($P<0.0001$, $n=360$, 1600–1959 AD)
MJ_40 ^[26]	0.58 ($P<0.0001$, $n=1742$, 220–1961 AD)
	0.76 ($P<0.0001$, $n=362$, 1600–1961 AD)
BO_40 ^[27]	0.78 ($P<0.0001$, $n=519$, 1422–1940 AD)
	0.88 ($P<0.0001$, $n=341$, 1600–1940 AD)

a) All curves are smoothed by 40-year moving average.

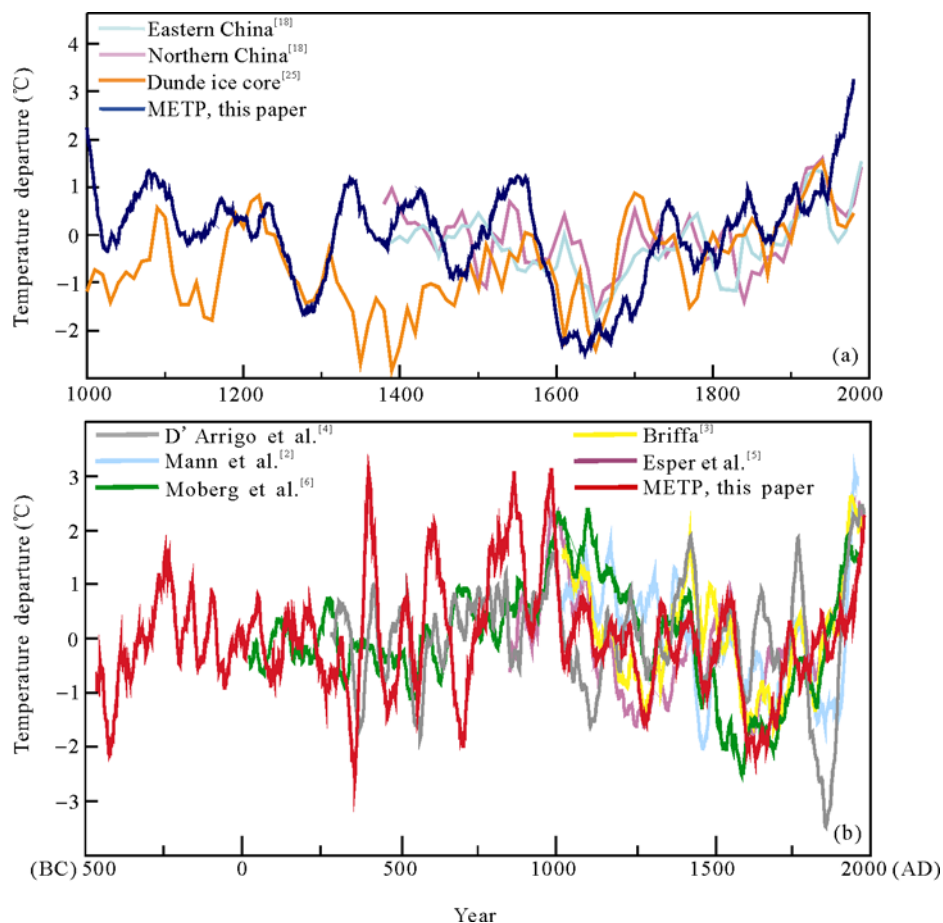


Figure 5 (a) Temperature comparisons among the mid-eastern Tibetan Plateau, northern and eastern China^[18], $\delta^{18}\text{O}$ of Dundee ice core^[25]. The mid-eastern Tibetan Plateau curve is smoothed by a 40-year moving average and others curves are every data for each decade. (b) The comparisons of temperature proxies among the mid-eastern Tibetan Plateau and other Northern Hemisphere scale. All curves are smoothed by a 40-year moving average.

violent fluctuations. It is most likely that the Tibetan Plateau amplified the temperature signals than other regions.

The mid-eastern Tibetan Plateau temperatures fluctuate gently around the mean, with a tendency to colder temperatures in the first centuries AD, until ca. 350 AD. This marks a transition to a ~700 year period of high inter-annual to multi-decadal variability in temperatures, and as a whole the period shows temperatures above average. It should be noted that some of the large variability from 784 to 989 AD may be due to fewer samples (Figure 4(a)). The second millennium AD shows the “Little Ice Age” (LIA) from about 16th to 19th centuries^[28], and also shows the unusual warming trend in the late of twentieth century.

Overall, in the mid-eastern Tibetan Plateau temperature record, five distinct warm and four distinct cold periods since 484 BC are evident (Table 7, Figure 4(b)). W1 (401–413 AD), W2 (604–609 AD), W3 (864–

882 AD), W4 (965–994 AD) and W5 (1970–2000) were the distinct warm intervals, where W1 to W4 were as warm as W5 or even warmer. C1 (348–366 AD), C2 (686–705 AD), C3 (1271–1296 AD) and C4 (1599–1702 AD) were the extreme cold periods, where C1 and C2 were colder than C4 which falls within the LIA.

However, we should view two periods, 450–485 BC and 864–882 AD, with caution. Because of fewer samples during those two periods, $\pm 2\sigma$ error bars show a large scale variations, the variability at the time could have been too high, which results in some uncertainty (Figure 4(b)).

2.2 Distinct cold periods

The tree ring based temperature variations are not only representative over the mid-eastern Tibetan Plateau, but also closely correspond to those of the north-central China to a certain extent over long time scales. It seems there is a relationship between the temperature varia-

Table 7 Distinct warm and cold intervals on the mid-eastern Tibetan Plateau during 484 BC–2000 AD and reconstructed temperature

Intervals	Time (a)	Mean temperature (°C)	Maximum temperature (°C)	Minimum temperature (°C)	σ
Distinct warm periods					
W1: 401–413 AD	13	2.89	3.25	2.46	0.26
W2: 604–609 AD	6	2.92	3.16	2.53	0.25
W3: 864–882 AD	19	2.8	3.43	2.0	0.4
W4: 965–994 AD	30	2.81	3.78	2.10	0.34
W5: 1970–2000 AD	31	2.73	3.26	1.83	0.36
Distinct cold periods					
C1: 348–366 AD	19	1.62	2.0	0.8	0.26
C2: 686–705 AD	20	1.71	2.3	1.33	0.27
C3: 1271–1296 AD	26	1.82	2.26	1.3	0.24
C4: 1599–1702 AD	104	1.77	2.37	1.1	0.27

tions and the dynasties downfall in China during the last 2485 years.

Historical data suggest that from the 1st to the 6th centuries (during the Eastern Han Dynasty, Three Kingdoms, Wei and Jin dynasties in China, see Figure 4(b)), China's climate was relatively cold^[29]. A great part of the mid-eastern Tibetan Plateau temperature record during this period is below the 485 BC–2000 AD mean. Because of the cold weather, grassland (pasture areas) extended to the south of the Yellow River, and the agricultural area retreated southwards during the Jin Dynasty. The whole northwestern China was dry and cold to an extent not previously experienced^[30]. The mid-eastern Tibetan Plateau temperature record suggests that during 348–366 AD temperatures were at their lowest for the last 2.5 millennia. It is quite similar to that Zhu's result^[29]. In this paper, our calculation shows that during 348–366 AD the mean temperature (mean 1.62°C for 19 years, and including minimum 0.8°C) was 1.11°C lower than that mean of 1970–2000 AD.

During the 11th and 12th centuries, the Song Dynasty, China again suffered an extremely cold period^[29,31], and the recorded severe cold period at the end of the 13th century during the Yuan Dynasty corresponds to C3 cold interval in the METP temperature curve. It was also cold in the 17th century, especially during the late 17th century^[29], corresponding to C4, the LIA. The LIA in the reconstruction appears to be synchronous with what has previously been reported for China in the literature^[29,31]. However, LIA, with mean temperature 1.77°C for 104 years, was not the coldest during the last 2485 years. C1 (1.62°C) and C2 (1.71°C) were colder than LIA. During the C4 cold period, Ming Dynasty was ruined and Qing Dynasty established.

It is striking that most major downfalls of Chinese

Dynasties were associated with low temperature intervals. Qin, Three Kingdoms, Tang, Song (North and South), Yuan, Ming and Qing dynasties ended in periods below average temperatures (Figure 4(b)). There were some lags in time for the downfalls of Han and Eastern Jin dynasties, but before their collapse, war had started during the low temperature intervals. For example, the Jin Dynasty ended in 420 AD, but historical documents^[29,31] show that chaos caused by war had already started in 386 AD (near to the lowest temperature, C1), and the Northern Dynasty started to establish in the same year. Possibly, the cold spell in the late 4th century played an important role in the Jin Dynasty's downfall. The Tang Dynasty's downfall in 907 AD also corresponds to a period of reduced temperatures compared with the warm periods before and after.

While the actual downfalls of dynasties may not be directly related to climate deterioration, it is probably the indirect effects of cold temperatures. For instance, low temperatures could lead to crop failure, resulting in famine that may breed uprisings and ultimately wars^[32,33]. Nomadic invasions and migrations to the south during these cold periods caused the pasture area to extend south^[30]. It is intriguing that the collapse of the Classic Maya civilization around 900 AD, which has been related to extensive and prolonged droughts^[34], coincides with the decline of the Tang Dynasty in China at around 907 AD^[22]. Thus, as Mesoamerican droughts have been found to coincide with cold Northern Hemisphere temperatures, it is an indication of the large-scale significance of the mid-eastern Tibetan Plateau temperature reconstruction.

2.3 Distinct warm periods

The warm period W1, between 401–413 AD, was the warmest period within the last 2.5 ka, and it is con-

spicuous not only because temperatures seemingly exceed those of today, but also because the swift shift from the very cold C1 phase to the warm peak W1 and subsequently rapid decline. This event falls within a part of the mid-eastern Tibetan Plateau tree-ring chronology where the reconstruction is quite reliable because it contains more than 160 tree samples. An archaeological documentary record^[35], from Loulan in Xinjiang province, shows that pomegranate, a vitamin-C rich fruit, was used as currency during the Eastern Jin Dynasty (317 to 589 AD). The appearance of pomegranate in high latitudes^[35] during the Eastern Jin Dynasty is an indication that temperatures at that time were higher than today. It is known that the efficient accumulated temperature (growing degree days) for pomegranate growth must exceed 3000°C, and the lowest temperature that leads to its death is -22°C to -20°C. The appearance of pomegranate during the Eastern Jin Dynasty suggests that the temperature at that time was higher than nowadays^[35].

W2 coincides with the peak of the short Sui Dynasty, and documentary evidence^[29] suggests that both the Sui and Tang (W3) dynasties were during warm periods in general, and that one kind of sub-tropical fruits, orange, could be planted in the northern city of Chang'an (now Xi'an). At present, this fruit cannot be planted in northern China due to the low temperature, indicating that the climate of Xi'an during the Sui and Tang dynasties was similar to that of lower latitudes in China today^[29,30]. Furthermore, during W2 and W3, climate in eastern China was warm, moist, and mild promoting palaeosol and lacustrine sediments to be developed in sandy areas so that previously shifting sands were fixed and vegetation cover increased^[36]. Both W3 and W4 occur in a period of predominantly above average temperatures in

the mid-eastern Tibetan Plateau, and it is interesting that the end of this warm period coincides with the start of the "Medieval Warm Period" (MWP)^[37] as seen in Europe (800–1300 AD), suggesting that the MWP was not a synchronous feature in the Northern Hemisphere. However, we should view W3 and W4 with caution as we mentioned above that there are fewer samples during those two periods.

The comparison between the mid-eastern Tibetan Plateau temperature record and CO₂ concentrations^[38] (estimated and observed) for the last millennium shows good agreement, where W5 coincides with the steep rise in CO₂ (Figure 6). In another word, W5 warm period may relate to CO₂ and other factors. However, CO₂ or other greenhouse gases cannot explain the warm periods W1 and W2 on the mid-eastern Tibetan Plateau since they occurred before the Industrial Revolution, suggesting that other factors caused those warm events. It is noteworthy that there are similar low-frequency variation trends between the METP temperature record and the solar output records (Figure 6)^[39]. It suggests that solar output is one of the driving forces of mid-eastern Tibetan Plateau temperatures, at least on long (>1000 years) timescales. Moreover, the high variability on the multi-decadal to centennial scale between 350 and 1000 AD in the mid-eastern Tibetan Plateau record is not visible in the solar output record (Figure 6), suggesting that other mechanisms caused those fluctuations. This needs more investigations.

In addition to providing the first annually resolved multi-millennial temperature reconstruction from Tibet, the mid-eastern Tibetan Plateau temperature record shows some features that raise questions about past climate variability in the region. The change to large amplitude in the multidecadal variability between 350 and

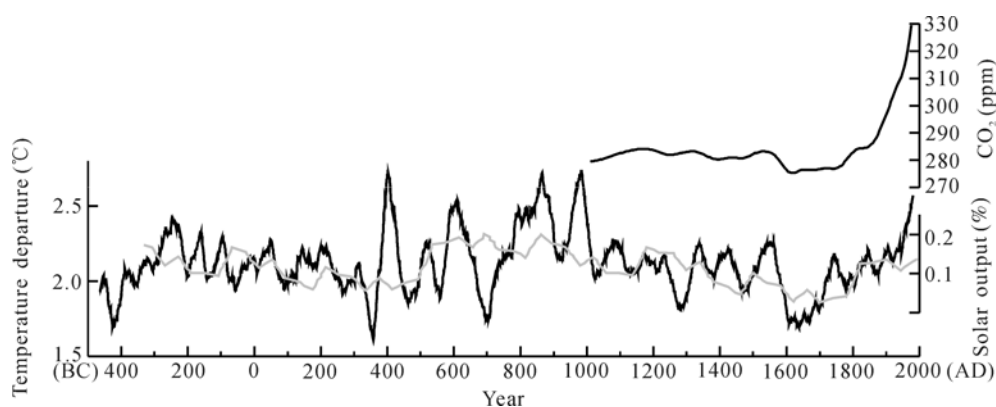


Figure 6 Comparison among CO₂ series (top)^[38], solar-output (gray line)^[39] and the mid-eastern Tibetan Plateau temperature (black line).

1000 AD needs to be further studied. Since it is not obvious in the other long temperature reconstructions in Figure 5(b), it may be a Tibetan Plateau regional feature, possibly related to large-scale circulation changes. The abrupt rise in temperature around 392 to 412 AD needs to be studied in detail. Similar features have been seen in tree-ring data from Mongolia^[4] and Fennoscandia^[40]. We named this abrupt change from cold (C1) to warm (W1) temperatures as the “Eastern Jin Event”, when the mean temperature suddenly increased from 1.62°C to 2.89°C. Due to the high replication at that time, we are confident that this significant and dramatic change existed. Future research will focus on finding the mechanisms behind this rapid temperature change and also set it in a modern context to find out whether there are any parallels to the present warming trends. Finally, we would like to note that in this paper we used the negative exponential curves or straight-lines to fit each ring-width measurement series during the detrending process. This could be possible limits in the low frequency signals. It could be potentially explored further in future with the use of different standardization approaches for extracting more low frequency information from these trees.

3 Conclusions

We conclude that the mid-eastern Tibetan Plateau temperature reconstruction can be regarded as being representative for north western as well as central-north China, possibly even on a hemispheric scale. During the last 2485 years, the period from 350 to 1000 AD stands out as a period of high-amplitude multidecadal temperature fluctuations. This period hosts four out of five periods of distinctly warm temperatures, as well as two of the four distinct cold periods. Our data suggests that the late twentieth century (1970–2000 AD) was the warmest during the last 1000 years. Uncertainty remains about the warm intervals between 780 and 890 AD due to low replication in the tree ring records. That of specific interest is the sharp rise in temperatures occurring in the late 4th century, the “Eastern Jin Event”. The change from very low to very high temperatures during that event is unprecedented in the last 2.5 ka. The twentieth century warming is much conspicuous in the mid-eastern Tibetan Plateau than in other regions in China since the 1950s.

We thank Tan L. C., Zhang Q. B., Ma L. M., Shi J. F., Yang Y. K., Wang L., Yi L., Li Q. and Ta W. Y. for their great help.

- 1 Jones P D, Briffa K R, Barnett T P, et al. High resolution paleoclimatic records for the last millennium: Interpretation, and comparison with circulation model control-run temperatures. *Holocene*, 1998, 8: 455–471
- 2 Mann M E, Bradley R S, Hughes M K. Northern Hemisphere temperatures during the past millennium: Inference, uncertainties, and limitations. *Geophys Res Lett*, 1999, 26: 759–762
- 3 Briffa K R. Annual climate variability in the Holocene: Interpreting the message of ancient trees. *Quat Sci Rev*, 2000, 19: 87–105
- 4 D’Arrigo R, Jacoby G, Frank D, et al. 1738 years of Mongolian temperature variability inferred from a tree-ring width chronology of Siberian pine. *Geophys Res Lett*, 2001, 28: 543–546
- 5 Esper J, Cook E R, Schweingruber F H. Low frequency signals in long tree-ring chronologies for reconstructing past temperature variability. *Science*, 2002, 295: 2250–2253
- 6 Moberg A, Sonechkin D M, Holmgren K, et al. Highly variable Northern Hemisphere temperatures reconstructed from low- and high-resolution proxy data. *Nature*, 2005, 433: 613–617
- 7 Osborn T J, Briffa K R. The spatial extent of 20th-century warming in the context of the past 1200 years. *Science*, 2006, 311: 841–844
- 8 Liu X D, Chen B D. Climatic warming in the Tibetan Plateau during recent decades. *Int J Climatol*, 2000, 20: 1729–1742
- 9 Zhang Q B, Chen G D, Yao T D, et al. A 2,326-year tree-ring record of climate variability on the northeastern Qinghai-Tibetan Plateau. *Geophys Res Lett*, 2003, 30: 1739–1742
- 10 Sheppard P R, Tarasov P E, Graumlich L J, et al. Annual precipitation since 515 BC reconstructed from living and fossil juniper growth of northeastern Qinghai Province, China. *Clim Dyn*, 2004, 23: 869–881
- 11 Bräuning A, Mantwill B. Summer temperature and summer monsoon history on the Tibetan Plateau during the last 400 years recorded by tree rings. *Geophys Res Lett*, 2004, 31, doi: 10. 1029/2004GL 020793
- 12 Shao X M, Huang L, Liu H B, et al. Reconstruction of precipitation variation from tree rings in recent 1000 years in Delingha, Qinghai. *Sci China Ser D-Earth Sci*, 2005, 48(7): 939–949
- 13 Liu Y, An Z S, Ma H Z, et al. Precipitation variation in the northeastern Tibetan Plateau recorded by the tree rings since 850 AD and its relevance to the Northern Hemisphere temperature. *Sci China Ser D-Earth Sci*, 2006, 49(4): 408–420
- 14 Liang E Y, Shao X M, Eckstein D, et al. Topography-and species-dependent growth responses of *Sabina przewalskii* and *Picea crassifolia* to climate on the northeast Tibetan Plateau. *Forest Ecol Manag*, 2006, 236: 268–277
- 15 Yang B, Bräuning A, Shi Y F. Late Holocene temperature fluctuations on the Tibetan Plateau. *Quat Sci Rev*, 2003, 22: 2335–2344
- 16 Gou X H, Chen F H, Yang M X, et al. Asymmetric variability between maximum and minimum temperatures in Northeastern Tibetan Plateau: Evidence from tree rings. *Sci China Ser D-Earth Sci*, 2008, 51(1): 41–55

- 17 Zhu H F, Zheng Y H, Shao X M, et al. Temperature variations during the last 1000 years recorded by tree ring for Wulan, Qinghai. *Chin Sci Bull*, 2008, 53(15): 1835—1841
- 18 Wang S W, Gong D Y, Zhu J H. Twentieth-century climatic warming in China in the context of the Holocene. *Holocene*, 2001, 11: 313—321
- 19 Dai J X. *Climate over the Tibetan Plateau, China*. Beijing: Meteorological Press, 1991. 1—356
- 20 Stokes M A, Smiley T L. *An Introduction to Tree-ring Dating*. Chicago: University of Chicago Press, 1968. 1—73
- 21 Cook E T, Kairiukstis L A. *Methods of Dendrochronology*. Holland: Kluwer Academic Publishers, 1990. 1—394
- 22 Xu X G. The discovery and research of Tubo tombs in Dulan, China. *Silk Road*, 2004, 14: 212—225
- 23 Efron B. Bootstrap methods: Another look at the jackknife. *Ann Stat*, 1979, 7: 1—26
- 24 Fritts H C. *Tree Ring and Climate*. London: Academy Press, 1976. 1—567
- 25 Thompson L G, Mosley-Thompson E, Davis M E, et al. Tropical glacier and ice core evidence of climate change on annual to millennial time scales. *Clim Change*, 2003, 59: 137—155
- 26 Mann M E, Jones P D. Global surface temperature over the past two millennia. *Geophys Res Lett*, 2003, 30: 1820—1823
- 27 Briffa K R, Osborn T J. Low-frequency temperature variations from a Northern tree ring density network. *J Geophys Res*, 2001, 106: 2929—2941
- 28 Bradley R S, Jones P D. ‘Little Ice Age’ summer temperature variations: Their nature and relevance to recent global warming trends. *Holocene*, 1993, 3: 367—376
- 29 Zhu K Z. The preliminary study on climatic variation of China for the last 5000 years. *Sci China*, 1973, 16: 168—189
- 30 Ni G J. Climatic variation and its impact to ancient agricultural economy over northern China. *Agric Archaeol*, 1988, 1: 294
- 31 Ge Q S, Zheng J Y, Fang X Q, et al. Winter half-year temperature reconstruction for the middle and lower reaches of the Yellow River and Yangtze River, China, during the past 2000 years. *Holocene*, 2003, 13: 933—940
- 32 Zhang D, Jin C Y, Lin C S, et al. Climate change, social unrest and dynastic transition in ancient China. *Chin Sci Bull*, 2005, 50(2): 137—144
- 33 Weiss H, Bradley R S. What drives societal collapse? *Science*, 2001, 291: 609—610
- 34 Gergana Y, Nowaczyk N R, Mingram J, et al. Influence of the inter-tropical convergence zone on the East Asian monsoon. *Nature*, 2007, 445: 74—77
- 35 Zhang X W, Zhang J B. *Handbook of Xinjiang Weather*. Beijing: Meteorological Press, 2006. 1—624
- 36 Wu J W, Lu R J, Zhao Y N. Sandy lands during the Medieval Warm Period in Eastern China. *Sci Soil Water Conserv*, 2004, 2: 29—33
- 37 Hughes M K, Diaz H F. Was there a ‘Medieval Warm Period’, and if so, where and when? *Clim Change*, 1994, 26: 109—142
- 38 Etheridge D M, Steele L P, Langenfelds R L, et al. Natural and anthropogenic changes in atmospheric CO₂ over the last 1000 years from air in Antarctic ice and firn. *J Geophys Res*, 1996, 101: 4115—4128
- 39 Charles A P, Kennen J H. Geophysical, archaeological, and historical evidence support a solar-output model for climate change. *Geophysics*, 2000, 97: 12433—12438
- 40 Linderholm H W, Gunnarson B E. Summer climate variability in west-central Fennoscandia during the last 3600 years. *Geogr Ann Ser A-Phys Geogr*, 2005, 87: 231—241